Structural transitions in a crystalline bilayer: the case of Lennard-Jones and Gaussian core models

Structural transitions in a crystalline bilayer: the case of Lennard-Jones and Gaussian core models

Tamoghna Das[1], **Surajit Sengupta**[1,2] **and Subhasis Sinha**[3]

[1] Department of Chemical, Biological and Macromolecular Sciences, S N Bose National Center for Basic Sciences, Block-JD, Sector III, Salt Lake, Kolkata 700098, India
[2] Centre for Advanced Materials, Indian Association for the Cultivation of Science, Jadavpur, Kolkata 700032, India
[3] Indian Institute of Science, Education and Research Kolkata, Block-HC, Sector-III, Salt Lake, Kolkata 700106, India

E-mail: tamoghna@bose.res.in

Abstract
We study structural transitions in a system of interacting particles arranged as a crystalline bilayer, as a function of the density ρ and the distance d between the layers. As d is decreased a sequence of transitions involving triangular, rhombic, square and centred rectangular lattices is observed. The sequence of phases and the order of transitions depends on the nature of the interactions.

(Some figures in this article are in colour only in the electronic version)

1. Introduction

Structural transitions in solids may be caused by various external parameters such as temperature, pressure, stress, electrical and magnetic fields [1, 2], etc. Confinement and dimensional reduction can also lead to structural transitions especially in soft solids like colloidal suspensions. Colloidal solids are especially suited to modification and manipulation using a variety of means such as structural confinement [3], laser-induced phase transitions [4], shear [5], static [6] and dynamic [7] external fields.

Confined colloids kept in a thin wedge geometry of two optically flat quartz glass plates exhibit a sequence of structural transitions: $n\triangle \to (n + 1)\square \to (n + 1)\triangle$ with increasing wedge height, where n is the number of layers and $\triangle$ and $\square$ correspond to layers of triangular ($p6$) and square ($p4m$) symmetry, respectively [8, 9]. The full equilibrium phase diagram of such a system has been studied analytically as well as using extensive computer simulations [10, 11]. The transitions are usually first order, though continuous transitions via a layer buckling mechanism [12] has also been predicted and observed.

In this paper, we explore another way in which structural transitions may be induced in a colloidal solid. Consider a crystalline bilayer separated by a distance d between the layers.

Each of these layers is held in place by individual trapping potentials, set up, for example, using laser tweezers [13]. The strong trapping potential ensures that out-of-layer fluctuations are typically unimportant. We investigate the stability of the bilayer as the distance d is decreased. We show that d behaves as a controlling parameter and induces a rich sequence of transitions involving a variety of two-dimensional Bravais lattices. The exact sequence of transitions crucially depends on the nature of interactions. In this paper we study two kinds of model solids: (a) the generic Lennard-Jones (LJ) [14] solid and (b) the soft Gaussian core model (GCM) [15] appropriate for suspensions of globular polymers. Our main results are as follows. For the LJ system, we obtain at temperature $T = 0$ two independent triangular (TRN) crystalline layers for large d. As d is reduced, the system undergoes a *first-order* transition to a staggered square (SQR) solid. This SQR solid continuously transforms to a TRN solid through a series of centred rectangular (CR) lattices with intermediate aspect ratios as d decreases to zero as the layers merge. Our calculations are therefore relevant for structurally confined simple soft solids where buckling transitions are suppressed due to a strong external trapping potential [3, 10, 11].

In contrast, for the GCM, *both* transitions are continuous. As d reduces, the TRN solid transforms to a SQR solid continuously through a sequence of rhombic (RMB) lattices.

The SQR solid subsequently transforms back to the TRN solid for small values of d, again continuously using a sequence of CR lattices. The progression of phases seen corresponds roughly with those seen in the extensive literature on classical interacting bilayer Wigner crystals [16], though the sequence of phases and the nature of transitions are different.

The rest of this paper is organized as follows. In section 2, we describe the bilayer system in detail, introducing the order parameters for the transition and state the interatomic potentials used. In section 3, we give the results for the zero-temperature energy minimization. This is followed in section 4 by a full normal mode analysis investigating the stability of the ground states obtained in section 3 and the nature of the transition. In section 5, we present results of finite temperature Monte Carlo simulations. We discuss our results and their implications and conclude in section 6.

2. Model system

Consider a system of $2N$ particles arranged as two parallel two-dimensional crystalline layers of N particles each (see figure 1). The crystal structure of each of these layers may be assumed to be a general two-dimensional oblique ($p2$) lattice. Each particle interacts with all other particles via isotropic and pairwise interacting potentials. The position vector for the ith particle of this lattice can thus be expressed as

$$\vec{r}_i = (m + \lambda)\vec{a} + (n + \lambda)\vec{b} + d\hat{z}$$
$$= ((m + \lambda)a + (n + \lambda)b\cos\phi)\hat{x} + (n + \lambda)b\sin\phi\hat{y} + d\hat{z}$$

$$(1)$$

where $m, n = 0, 1, 2, \ldots$, $\vec{a}$ and $\vec{b}$ are two in-plane basis vectors, ϕ is the angle between these two basis vectors, d is the inter-layer separation and λ is a shift between the centre of masses of two layers (figure 1). Therefore to specify our model completely, knowledge of these five variables, a, b, ϕ, d, λ is sufficient. The last variable λ ensures that, for small values of d, the particles from different layers do not overlap. The particles are not allowed to fluctuate out of the layers and particle exchange between the layers is prohibited. Each layer is therefore considered to be strongly confined in the $\hat{z}$ direction while they are allowed complete freedom in the x, y plane.

Let us first imagine the possible physical scenario as the layers are brought close to each other starting from a large inter-layer separation. When the layers are well apart they exist as two independent monolayers and they show TRN symmetry, the minimum energy configuration for the two-dimensional crystalline system for the interaction potentials considered by us. As the inter-layer separation, d, between these two layers starts decreasing, the system passes through a series of structural transitions which may involve RMB and SQR phases. For even smaller values of d, two layers start merging into one and the TRN symmetry is regained. Transformation between an SRQ and a TRN phase may be accomplished, in general, by either (i) shear, i.e. change in the angle between two in-plane basis vectors producing an intermediate RMB structure, or (ii) change in the aspect ratio (b/a) which produces a CR lattice. Both the RMB and the CR
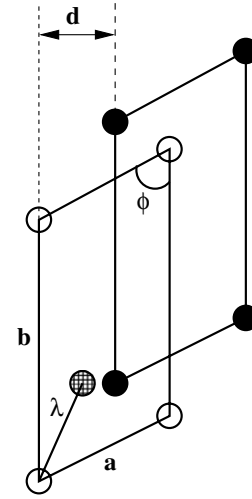

Figure 1. A schematic diagram of the model bilayer solid explaining the structural parameters. The crystal structures on each of the layers, denoted by filled and open circles, are identical but staggered by the amount λ along the diagonal. The lattice parameters are a and b and the apex angle is ϕ. The half-filled circle is the projection of a lattice point (filled circle) on the top layer to the bottom one.

lattices being less symmetric have TRN and SQR phases as limiting cases.

It is therefore clear that we need to introduce two order parameters [17] in order to describe completely the phase transitions of our model system. First, the bond angle order parameter $\psi = \cos\phi$ which is 0 when the system takes SQR symmetry ($\phi = 90°$) and non-zero otherwise. The second-order parameter ξ is related to the aspect ratio b/a as $\xi = (b/a - 1)/(\sqrt{3} - 1)$ which varies from 0 in the SQR to a non-zero value in the CR phase. Note that the highly symmetric TRN phase is described both by ($\psi = 0.5, \xi = 0$) and ($\psi = 0.0, \xi = 1$). Finally, if $\epsilon_{ij}, i, j = x, y$ is the two-dimensional strain tensor, the shear, $e_3 = \epsilon_{xy}$, and deviatoric, $e_2 = \epsilon_{xx} - \epsilon_{yy}$, strains are related to ϕ and ξ as

$$\tan\phi = \epsilon_3/(1 - \epsilon_1)$$
$$\xi = \frac{2(1 + \epsilon_2) + \epsilon_1}{2(1 - \epsilon_2) + \epsilon_1}.$$

$$(2)$$

We have studied phase transitions in the bilayer system for two different model potentials. The Lennard-Jones potential:

$$U = \sum_{i \neq j} V_{LJ}(r_{ij}) = 4\epsilon\left[\left(\frac{\sigma}{r_{ij}}\right)^{12} - \left(\frac{\sigma}{r_{ij}}\right)^6\right]$$

$$(3)$$

has been used extensively in the past as a generic model which includes both long range attractive and short range repulsive interactions. In equation (3), $r_{ij} = |\vec{r}_i - \vec{r}_j|$, the distance between the i and jth particle. An intrinsic length scale $r_{min} = 2^{1/6}\sigma$ corresponding to the minimum of V_{LJ} may be associated with this potential. The nearest-neighbour distance between particles is close to this value throughout. We use reduced units for the LJ potential throughout the paper defining lengths in units of σ and energy in units of ϵ. It follows that the

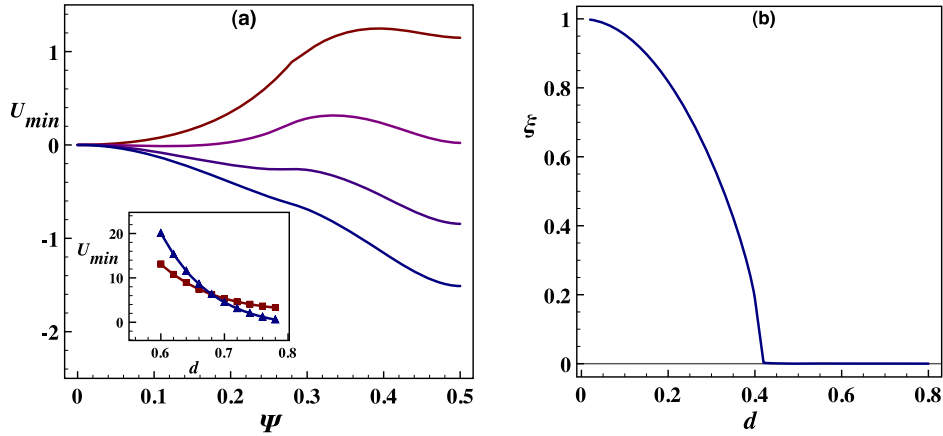**Figure 2.** (a) Plots of the total energy as a function of ψ at $\rho = 1.2$ and (top to bottom) $d = 0.66, 0.68, 0.70$ and 0.72 showing the SQR to TRN transition for the LJ system. Inset: the energies of the SQR (filled square) and TRN (filled triangles) plotted as a function of d are seen to cross with a change in slope as expected of a first-order transition. The fact that this transition is first order has also been verified by a normal mode analysis. (b) Plot of the order parameter ξ as a function of d at the same density showing the continuous transition SQR $\rightarrow$ TRN as $d \rightarrow 0$. The lattices with intermediate ξ have CR symmetry.

densities are in units of σ^{-2} and temperatures in units of ϵ/k_B, where k_B is the Boltzmann factor.

On the other hand, the *Gaussian core* potential has been used specifically to model soft solids:

$$U = \sum_{i \neq j} V_{GCM}(r_{ij})$$
$$= \sum_{i \neq j} V_0 \exp[-(r_{ij}/l)^2], \qquad V_0, l > 0 \qquad (4)$$

V_0 and l acts as the energy and length scales for this potential and r_{ij} is the same as it was for the previous equation. The GCM is interesting because, firstly, the potential is soft and is known to display behaviour similar to that of real polymeric solids. Also, many of its properties are well known and tested especially because at very low densities it reduces to the hard disc model which is widely used for modelling colloidal solids. Due to the purely repulsive nature of this potential, it does not have any preferred nearest-neighbour distance which is determined in this case by the density. This potential also possesses an interesting duality property [18] such that high ($\rho_>$) and low ($\rho_<$) density properties are related to each other by

$$\rho_> \rho_< = \pi^{-D} \qquad (5)$$

where D is the dimensionality. It is therefore sufficient to confine our studies in the range $0 < \rho < \rho_{f.p.}$ where the fixed point density $\rho_{f.p.} = \pi^{-1} \simeq 0.32$ in two dimensions.

3. Zero-temperature calculation

In this section, we determine the ground states of our system in the space of the order parameters, ϕ and ξ, keeping the layer separation d and the density ρ as external parameters. Below we discuss our results for the LJ solid and the GCM one after the other.

3.1. Lennard-Jones potential

We begin with $2N$ particles divided into two layers, each arranged in a TRN lattice of N particles. For a fixed layer separation d, and the lattice parameter a set by the density ρ, we minimize the total energy U with respect to λ and b. The resulting order parameter ξ remains constant at 1—the value appropriate for the TRN lattice. For the lattice sums needed to calculate the minimized energy we have set a cutoff radius, $r_c = 2.5\sigma$.

In figure 2(a) we have plotted the minimized energy U_{min} as a function of the order parameter ψ for various values of d. For large inter-layer separation, the bond angle order parameter at the minimized energy (U_{min}) shows a non-zero value, $\psi = \cos\phi = 0.5$, which indicates TRN symmetry ($\phi = 60°$). The minimum in λ is very shallow indicating two triangular lattices prefer to remain independent. As d is decreased two layers fall into registry and for a further decrease of d a second minimum at $\psi = 0$ develops, corresponding to the SQR phase ($\phi = 90°$). A plot of the energy of the SQR and TRN phases (figure 2(a) inset) shows a first-order transition at $d = 0.684$. This fact is confirmed by a normal mode analysis presented in section 4.

At even smaller values of d, the square solid begins to deform continuously by changing the aspect ratio (or order parameter ξ) at fixed ϕ. In figure 2(b) we have plotted the minimized value of ξ versus d. From the plot it is obvious that there is a continuous transition taking the solid from SQR at $\xi = 0$ to an eventual TRN phase at $\xi = 1$ via an intermediate CR lattice of $0 < \xi < 1$.

3.2. Gaussian core model

Due to the purely repulsive nature of the Gaussian core potential, it does not have any preferred nearest-neighbour distance and the solid would disintegrate unless confined in all directions. We have carried out all minimizations for a system with fixed reduced density, $\rho = 0.2$. We have plotted the
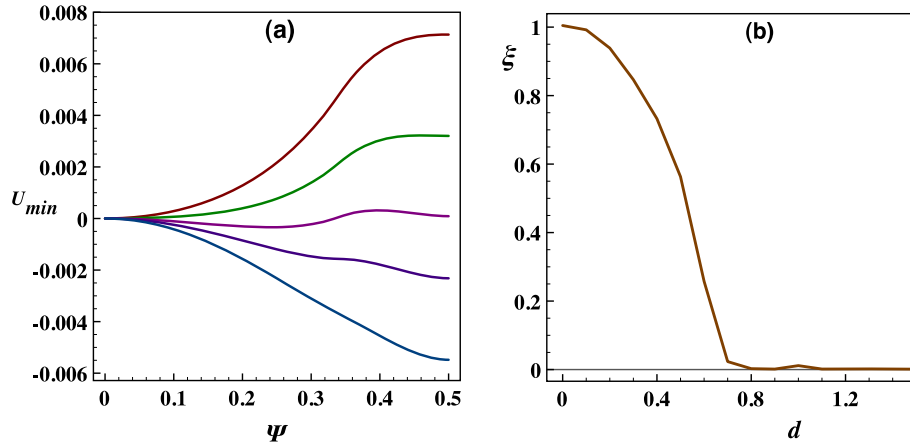
Figure 3. (a) Plot of the total energy in the GCM for $\rho = 0.2$ and (top to bottom) $d = 1.4, 1.5, 1.6, 1.7$ and 1.9 as a function of ψ. Note the appearance of the minimum at $\psi = 0.5$ corresponding to the TRN lattice as d increases. (b) The continuous transition from the SQR to the TRN lattice as $d \to 0$.
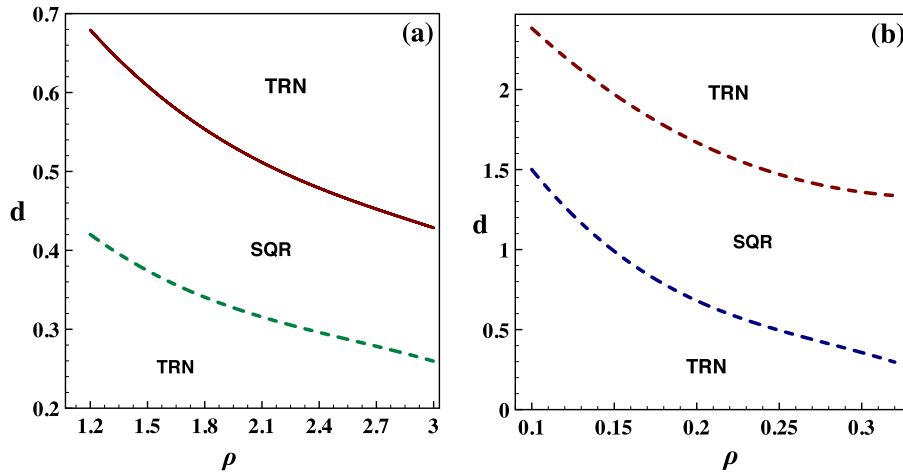

Figure 4. Zero-temperature phase diagrams in the ρ–d plane for the LJ (a) and GCM (b) systems. The various phases are marked. First-order transitions are shown by solid lines and continuous transitions by dashed lines.

minimized energy $U_{\min}$ as a function of the bond angle order parameter ϕ for various values of d. In figure 3(a) in contrast to the Lennard-Jones solid we now obtain continuous transitions from TRN to SQR through a set of RMB phases and back to TRN at $d = 0$ through a set of CR phases.

Our results concerning the various ground states and structural transitions in both the LJ and GCM systems in the ρ–d plane have been shown in the zero-temperature phase diagrams, figures 4(a) and (b), respectively. Note that for both systems the triangular phase is stable at all ρ for both very large d and $d = 0$ where the system becomes effectively two-dimensional.

4. Normal mode analysis

To further characterize the structural transitions in the two systems, we have undertaken a normal mode analysis [19] of the TRN and SQR solids obtained for each of the two interactions.

Let $\vec{u}(\vec{r}_i)$ be the displacement of the ith particle from its equilibrium position $\vec{r}_i$. Within the harmonic approximation, now the potential can be written as

$$U_{\text{harm}} = \frac{1}{2} \sum_{i,j} \vec{u}(\vec{r}_i) \mathcal{D}(\vec{r}_i - \vec{r}_j) \vec{u}(\vec{r}_j) \tag{6}$$

$$\mathcal{D}(\vec{r}_i - \vec{r}_j) = D_{\mu\nu}(\vec{r}_i - \vec{r}_j)$$
$$= \delta_{\vec{r}_i \vec{r}_j} \sum_k V_{\mu\nu}(\vec{r}_i - \vec{r}_k) - V_{\mu\nu}(\vec{r}_i - \vec{r}_j) \tag{7}$$

where $V_{\mu\nu}(\vec{r}) = \partial^2 V / \partial r_\mu \partial r_\nu$. We have $2N$ equations of motion, one for each of the three components of the N particles, since we have already restricted fluctuation in the z direction:

$$\ddot{\vec{u}}(\vec{r}_i) = -\sum_j \mathcal{D}(\vec{r}_i - \vec{r}_j) \vec{u}(\vec{r}_j). \tag{8}$$

We seek solutions to the equations of motion in the form of simple plane waves:

$$\vec{u}(\vec{r}, t) = \vec{\epsilon} \exp[i(\vec{k} \cdot \vec{r} - \omega t)]. \tag{9}$$
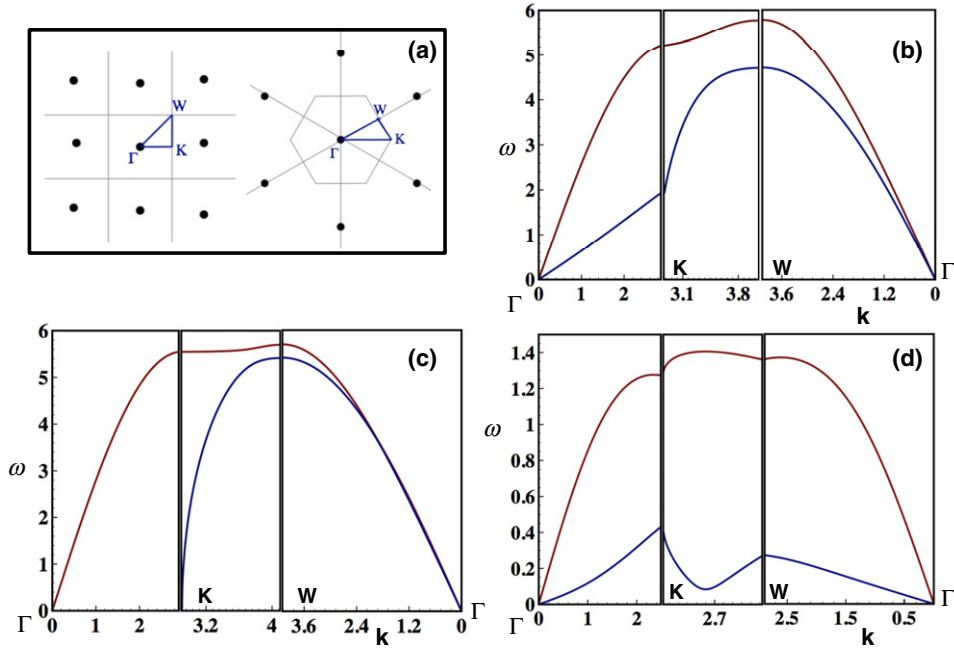
Figure 5. Results for phonon dispersion curves: (a) diagram showing the high symmetry points in the SQR and TRN (reciprocal) lattices. (b) Phonon dispersion for the stable SQR lattice at $\rho = 1.2$ and $d = d_c = 0.684$, i.e. the value of d at SQR to TRN transition. Note that the dispersion curve shows that the SQR phase is locally stable pointing to a first-order transition. (c) Phonon dispersion of the SQR solid at $\rho = 1.2$ and $d = 0.4$ showing an instability in the transverse acoustic branch. At this value of d a CR solid is stable. (d) Dispersion curve for the TRN solid in the GCM for $\rho = 0.2$ and $d = 1.6$ showing the appearance of a non-zero k vector soft mode.

Here $\vec{\epsilon}$ is the *polarization vector* of the normal mode. The *Born–von Karman* periodic boundary conditions restricts the wavevector $\vec{k}$ to a single primitive cell of the reciprocal lattice vector, which is normally identified with the first Brillouin zone.

Substituting equation (8) into equation (7) we find a solution of the three-dimensional eigenvalue problem:

$$\omega^2 \vec{\epsilon} = \mathcal{D}(\vec{k})\vec{\epsilon}. \tag{10}$$

Here $\mathcal{D}(\vec{k})$, the *dynamical matrix*, is given by

$$\mathcal{D}(\vec{k}) = \sum_i \mathcal{D}(\vec{r}_i) e^{-i\vec{k}\cdot\vec{r}_i}. \tag{11}$$

Two solutions to equation (9) for each of the N allowed values of $\vec{k}$ give us $2N$ normal modes. The reciprocal lattices for both SQR and TRN are known to have the same symmetry of the real space lattice. Exploiting this property, one finds the values of ω only for those k values along the lines connecting the high symmetry points of the first Brillouin zone (figure 5(a)), thereby obtaining the dispersion curve ω versus $|\vec{k}|$ and mode structure of a given lattice. For any stable equilibrium structure ω should always be non-negative definite.

4.1. The Lennard-Jones potential

To show that the SQR $\rightleftharpoons$ TRN transition at large d is indeed first order, we have obtained the dispersion curves for the metastable SQR phase for a value of d slightly larger than the critical $d_c = 0.684$ for the chosen $\rho = 1.2$. This is shown in figure 5(b). This indicates that the transition is first order with the possibility of coexistence. When d is decreased further, ψ at the minimized energy $U_{\min}$ shows minima at $\psi = 0$ but the normal mode analysis shows us that the SQR structure cannot be stable at this value of d (figure 5(c)). Actually, the two layers start merging into one by changing the aspect ratio away from $b/a = 1$.

4.2. The Gaussian core model

For the Gaussian core model the scenario is quite different. For intermediate values of d, the SQR structure is seen to be unstable and the mode structure for the TRN structure exhibits *mode softening*, figure 5(d), such that $\omega \rightarrow 0$ for $k \neq 0$. Examination of the deformation corresponding to this $\vec{k}$ shows that the SQR lattice becomes unstable to shear deformation at the zone boundary. This mode softening therefore establishes the transition from the TRN to SQR transition to be continuous for the Gaussian core model.

The transition from SQR back to TRN at low d is always continuous both for LJ and GCM as verified by our normal mode analysis.

5. Finite temperature results

We close our discussion on structural transitions in a bilayer crystal by briefly mentioning some of our results for the LJ case using Monte Carlo simulations [20]. A detailed calculation of the phase diagram of the bilayer GCM in the temperature, ρ and d space using both Monte Carlo and classical mean field
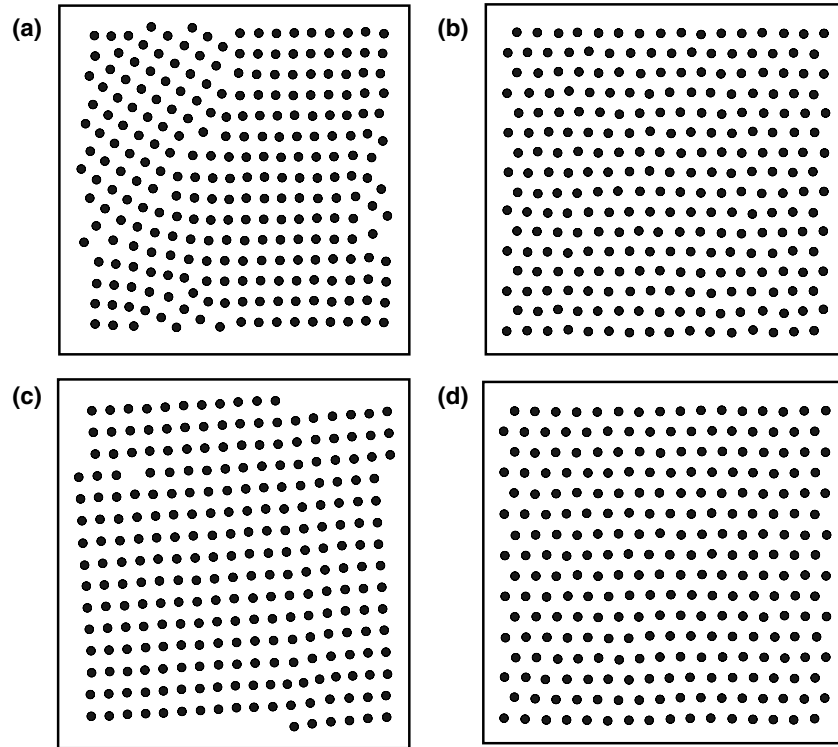
Figure 6. Configurations from our Monte Carlo simulation in the LJ system for $T = 1.0$. (a), (b) Show the result of increasing d from $d = 0.6$ to 0.8 at fixed $\rho = 1.20$. Note the first-order SQR to TRN transition. (c), (d) Show the corresponding result for pressure-induced SQR to TRN transition as ρ is increased from 1.3 to 1.4 at fixed $d = 0.6$. Our results are consistent with those seen in figure 4(a).

density functional theory, which is known to yield particularly good results for this system, will be published elsewhere.

The simulation is done using the usual Metropolis algorithm keeping the total number (N) of particles, volume (V) and temperature (T) fixed. Periodic boundary conditions have been used for all directions except in the direction of stacking of the layers. For our purpose, we use a system of 512 number of particles, temperature is fixed at 1.0 and the volume is determined by the density, $\rho = 1.2$, used for simulation. Starting from a large layer separation ($d \gg 0$), we have observed (see figure 6) the system change its symmetry from TRN to SQR with decreasing d. For large values of d ($d > 0.8$), when the two layers are well separated, each layer behaves independently of each other, exhibiting the expected TRN structure. As d is decreased, the two layers start interacting with each other. As a result, part of the system starts to transform into a SQR. Through this phase coexistence, the whole system transforms to a state where each layer shows SQR structure at $d = 0.6$.

We have also explored the configurations of our model system in the temperature–density plane keeping the inter-layer separation fixed. For $d = 0.6$, where we have already seen the SQR structure to be the ground state, we increase ρ to 1.3. We again encounter a first-order boundary and the system equilibrates to the SQR structure.

The values of the critical d and ρ compare favourably with the $T = 0$ phase diagram shown in figure 4(a). Similar scans at other temperature values over a large range of ρ and d have confirmed that it is not possible to induce a structural transition
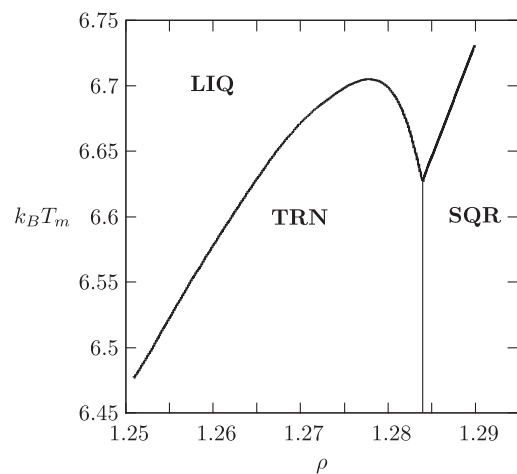

Figure 7. The melting curve $k_B T_m$ as a function of the reduced density ρ showing TRN and SQR lattices as well as the liquid (LIQ) phase for the LJ system. The melting points for each structure were obtained within a simple Lindemann parameter analysis [16] with the reduced root-mean-squared displacement of a particle assumed to be ≈ 0.1 times the lattice parameter at melting. The value of d is taken as 0.4. The melting temperature reduces sharply with d approaching the value at two dimensions $d \rightarrow \infty$.

in this model by changing T. The phase boundaries shown in figure 4 therefore extend vertically up to a melting temperature $T_m(\rho, d)$ (see figure 7). This behaviour is identical to that seen in the classical Wigner crystal and is probably an universal feature of such crystalline bilayers.

6. Summary and conclusion

In this paper we have studied structural transitions in a bilayer crystal. We have shown that the system has a rich phase diagram and shows a number of phase transitions. The identity of the phases and the nature of the transitions depend on the interaction potential. On the other hand, some features of these transitions, e.g. the overall topology of the phase diagram, seems to be similar and independent of the details of the interaction.

We believe that it may be easy to realize this soft matter system experimentally and study many of its interesting equilibrium and dynamic characteristics. For example, critical properties of the continuous structural transitions, especially near the melting line, and a detailed study of finite size scaling and crossover in these systems may be illuminating [21]. We are also particularly interested in the dynamics of the structural transitions for both the first-order and continuous cases. Quenches from the SQR to the TRN lattice in this system may be accomplished simply by changing d. How does the new phase form inside the parent? Is there a possibility of a martensitic transition [22, 23]? If so, then of what type? We hope our work stimulates experiments designed to answer these questions in the near future.

References

[1] Chen *et al* 1992 *Phys. Rev. Lett.* **69** 688
[2] Wen *et al* 1999 *Phys. Rev. Lett.* **82** 4248
[3] Schmidt M and Löwen H 1996 *Phys. Rev. Lett.* **76** 4552
[4] Chaudhuri D and Sengupta S 2006 *Phys. Rev.* E **73** 011507
[5] Steveno M J, Robbins M O and Belak J F 1991 *Phys. Rev. Lett.* **66** 3304
[6] Chaudhuri A, Sengupta S and Rao M 2005 *Phys. Rev. Lett.* **95** 266103
[7] Sengupta A, Sengupta S and Menon G I 2007 *Phys. Rev.* B **75** 180201(R)
[8] Pirenski P, Strzelecki L and Pansu B 1983 *Phys. Rev. Lett.* **50** 900
[9] Neser S, Bechinger C, Leiderer P and Palberg T 1997 *Phys. Rev. Lett.* **79** 2348
[10] Fortini A and Dijkstra M 2006 *J. Phys.: Condens. Matter* **18** L371
[11] Ghatak C and Ayappa K G 2002 *J. Chem. Phys.* **117** 5373
[12] Chou T and Nelson D R 1993 *Phys. Rev.* E **48** 4611
[13] Metcalf H J and van der Straten P 1999 *Laser Cooling and Trapping* (Heidelberg: Springer)
[14] Phillips J M, Bruch L W and Murphy R D 1981 *J. Chem. Phys.* **75** 5097
[15] Stillinger F H and Weber T A 1981 *J. Chem. Phys.* **74** 4015
[16] Goldoni G and Peeters F M 1996 *Phys. Rev.* B **53** 4591
Schweigert I V, Schweigert V A and Peeters F M 1999 *Phys. Rev.* B **60** 14665
Schweigert I V, Schweigert V A and Peeters F M 1999 *Phys. Rev. Lett.* **82** 5293
[17] Hatch D M, Lookman T, Saxena A and Stokes H T 2001 *Phys. Rev.* B **64** 060104(R)
[18] Stillinger F H 1979 *Phys. Rev.* B **20** 299
[19] Ashcroft N W and Mermin N D 1976 *Solid State Physics* (Philadelphia, PA: Saunders)
[20] Frenkel D and Smit B 2002 *Understanding Molecular Simulation: from Algorithm to Applications* (New York: Academic)
[21] Chaikin P M and Lubensky T C 1995 *Principles of Condensed Matter Physics* (Cambridge: Cambridge University Press)
[22] Bhattacharya J, Paul A, Sengupta S and Rao M 2008 *J. Phys.: Condens. Matter* **20** 365210
[23] Paul A, Bhattacharya J, Sengupta S and Rao M 2008 *J. Phys.: Condens. Matter* **20** 365211